Journal of Global Economic Analysis, Volume 8 (2023), No. 1, pp. 21-54.

A Latin Hypercube Sampling Utility: with an application to an Integrated Assessment Model

BY DOMINIQUE VAN DER MENSBRUGGHE[a]

This paper describes the use of a utility that creates a Latin Hypercube Sample (LHS). The LHS approach to sampling has had wide applicability as it represents a Monte Carlo strategy that limits sample size and therefore computer time to study the outcomes of simulations under uncertainty. Other approaches to deal with the 'size' problem include Gaussian Quadrature (GQ) (Arndt, 1996), often used in the context of large models such as computable general equilibrium models. However, the GQ approach is most suitable for focusing on a small set of uncertain parameters as the number of model evaluations increases substantially with the number of uncertain parameters and/or the moments to track. The utility is a new version of the LHS utility that has been publicly available from Sandia National Labs since the early 2000s. Beyond the recoding from FORTRAN to C/C++, the new version of the utility has some additional features including new output options and additional statistical distributions. This paper demonstrates the use of the new utility by coupling it to an integrated assessment (IAM) model which is derived from the META 21 model developed by Dietz et al. (2021). The META 21 model has many components that can be readily integrated into global economic models that track greenhouse gas emissions—a simple climate module, economic impacts derived from sea-level and temperature rises and bio-physical tipping points such as the Amazon dieback. The IAM results suggest that the social cost of carbon increases by an average of around 26% when taking into account the tipping points and that the tipping points lead to an additional decline of 0-5% in per capita consumption in 2100 on top of the other damages related to climate change. The utility and the code to the IAM model are available as supplementary materials.

JEL codes: C15, C65, O44, Q51, Q54

Keywords: Monte Carlo, Latin Hypercube Sampling, Integrated Assessment

[a]The Center for Global Trade Analysis, Department of Agricultural Economics, Purdue University, West Lafayette, IN, USA. Corresponding e-mail: vandermd@purdue.edu

1. Introduction

This paper describes the use of a utility that creates a Latin Hypercube Sample (LHS). The LHS approach to sampling has had wide applicability as it represents a Monte Carlo strategy that limits sample size and therefore computer time to study the outcomes of simulations under uncertainty.

The LHS approach combines two features. The first is that the sampling domain is segmented into equal lengths, which guarantees that the full domain will be sampled from—unlike the unrestricted Monte Carlo sampling approach. The second is that the sample is ordered such that it is close to a desired correlation matrix across the full or subset of sampled variables, which may be derived from statistical estimation. In the absence of a user-specified correlation, the approach assumes that the sampled variables are uncorrelated.

In the realm of large, complex and non-linear economic models such as computable general equilibrium (CGE) or more broadly, integrated assessment models (IAM), one alternative to Monte Carlo-type simulation has been the Gaussian Quadrature (GQ) approach to approximate the uncertainty bands for key model results (Arndt (1996), DeVuyst and Preckel (1997) and Pearson and Arndt (2000)). This approach is particularly useful for assessing the uncertainty of model results for a limited number of uncertain parameters and tracking a limited number of moments. The upper bound on the number of simulations (or points) needed for the GQ approach is given by:[1]

$$\bar{J} = \begin{pmatrix} N+M \\ M \end{pmatrix}$$

where N is the number of random variables and M is the order of the quadrature—typically 3.[2] With 5 uncertain variables the upper bound is 56 points for an order 3 GQ estimation, but this jumps to 1,771 for 20 uncertain variables. The number of required points rises rapidly for higher orders, for example to over 10,000 for 20 uncertain variables and order 4. Villoria and Preckel (2017) argue that using order 3 approximation leaves out significant information on the underlying distribution, for example skewness. The IAM used in this paper has 582 uncertain parameters, which for an order 3 GQ approach would require over 33 million points. The sampling strategy for the IAM uses a wide mix of distributions—some of which are far from symmetric and also incorporates a number of desired correlations, so an order 4 approach is probably necessary to capture the higher moments. For this, the GQ approach would require over 4 billion points. Even if the uncertainty is limited to a subset of the parameters, the number of points needed for an order 4 approach

[1] Villoria and Preckel (2017)

[2] Order 3 insures that the approximation is good for the first 2 moments of the underlying distribution.

would be prohibitive. Moreover, the IAM has other uncertain processes related to the tipping points, which are not subject to the same sampling approach as the uncertain parameters. The LHS approach also has the benefit of being straightforward to implement. Finally, the availability of parallelization has taken some 'sting' out of the 'size' problem, even on desktop computers. Villoria (2017) demonstrated the benefit of parallelization with an application of Monte Carlo simulations with the GTAP model. In that study, parallelization was implemented using a script in R. The Monte Carlo simulations in this study use a script in Python (van der Mensbrugghe, 2023c), which can be readily adapted to other contexts. For this study, parallelization reduced the compute time of the 20,000 simulations from 7-9 hours to 50-60 minutes on a relatively new and well-equipped desktop computer running under Windows.

The LHS utility described herein is a new version of the LHS utility that has been publicly available from Sandia National Labs (Swiler and Wyss, 2004) since the early 2000s. Beyond the recoding from FORTRAN to C/C++, the new version of the utility has some additional features including new output options and additional statistical distributions.

This paper demonstrates the use of the new utility by coupling it to an integrated assessment (IAM) model which is derived from the META 21 model developed by Dietz et al. (2021). The META 21 model, beyond demonstrating the LHS approach to taking into account uncertainty, also has many components that can be readily integrated into global economic models that track greenhouse gas emissions—a simple climate module, economic impacts derived from sea-level and temperature rises and bio-physical tipping points such as the Amazon dieback. The utility and the code to the IAM model are available as supplementary materials.

The LHS utility has been compiled as a stand-alone 'exe' file for Windows-based computers,[3] and can readily be embedded in a complex workflow. It has five output options for the sample: (1) a 'CSV' file; (2) an 'XML' file, which is ready for use in Excel; (3) a 'GMS' text file for GAMS; (4) a 'GDX' file, also for use with GAMS; and (5) the original file format of the FORTRAN code. The LHS utility includes over 40 statistical distributions and the ability to impose a correlation relation across two or more of the sampled variables. A summary user guide is available (van der Mensbrugghe, 2023b) and is meant to document this version of the LHS utility— and for most users should be sufficient—, but the more complete documentation is available in Swiler and Wyss (2004), save for the new features included with this version of the LHS utility.

A subsequent section illustrates the use of the LHS utility by coupling it to a relatively recent integrated assessment model (IAM) called META 21 (Dietz et al. (2021)), which has a focus on a number of potential bio-physical tipping points,

[3]The C/C++ code is intended to be fully ANSI compatible and should compile readily on UNIX-based computers including the Macintosh operating system.

which can be generated by rising temperatures. This paper only highlights two modules of the META 21 model to demonstrate the LHS utility, though the results section relies on the full model. Many components of META 21 can be readily ported to global CGE models that generate greenhouse gas emissions—emissions are (nearly) exogenous in Meta 21. Like with most IAMs, emissions lead to changes in the carbon cycle (including atmospheric chemistry), which generates changes to radiative forcing and temperature, which then leads to impacts—for example on GDP, and, in the case of META 21, bio-physical tipping points. In addition to demonstrating the utility of the LHS approach to Monte Carlo-type sensitivity analysis, the META 21 model also shows how to incorporate random events in model simulations. In META 21 these are related to the start of tipping points, but many examples abound in economics such as recessions, pandemics, natural catastrophes, conflicts, etc. Integrating extreme events in complex CGE models is a challenge for a number of reasons: (1) availability of historical data to estimate probabilities of the extreme events; (2) the need for assumptions on how the probabilities evolve over time; (3) the evolution of vulnerable populations based on demographics, migration, education, income and sources of livelihood; (4) assessing the economic impacts of the event; (5) integrating a typically local event into a typically aggregate model; and (6) running forward looking simulations enough times to capture the stochasticity of the event. Pauw et al. (2011) is an example of a study that has assessed some of these issues in the context of a country-based CGE model—extreme weather events in Malawi. Fernando, Liu, and McKibbin (2021) provides a summary of linking extreme events to economic potential and describes and summarizes one of the key global databases for evaluating weather-based extreme events.

The original implementation of META 21 is an Excel file coupled to an Excel add-in known as @Risk, which uses the same type of sampling methodology as the LHS utility.[4] This paper uses a re-coded GAMS version of META 21, that has been thoroughly tested and is able to re-produce the Excel version results.[5] The GAMS code is available in the supplemental materials. The final section describes how to couple the LHS utility with the IAM and highlights some of the key findings from the uncertainty analysis. Large parts of the GAMS version of the META 21 code can be ported almost directly into GAMS-based economic models of climate change. For example, the ENVISAGE[6] model has been using the same carbon cycle and energy balance components of META 21 and could be readily augmented with one or more of the tipping point components. Similarly, ENVISAGE has climate-related economic impacts—though using a bottom-up approach rather than the top-down approach in META 21. The challenge for models like ENVISAGE is the limits to

[4] Available at https://github.com/openmodels/META-2021

[5] In the deterministic version as the stochastic results are likely to differ.

[6] van der Mensbrugghe (2019)

Monte Carlo simulations, even with parallelization. A single suite of 10,000 simulations of the META 21 model takes 25-30 minutes, which is about the amount of time for a single dynamic run of the ENVISAGE model.

2. Latin Hypercube Sampling

2.1 An introduction to Latin Hypercube Sampling

Monte Carlo methods are well established techniques to explore model or simulation uncertainty when the underlying model is based on uncertain parameters (but with an assumed distribution). For each uncertain parameter, a draw of a random deviate is taken from the known distribution—and if there are k uncertain parameters, each draw will consist of selecting a random deviate for each of the k uncertain parameters. Latin Hypercube Sampling (LHS) (McKay, Beckman, and Conover, 1979) was introduced as an efficient sampling method, where efficiency allows for limiting the size of the sample while at the same time insuring that the entire sample space is covered.

Before explaining LHS, we describe first the technique for generating random deviates. If a distribution has an easily invertible cumulative distribution function (CDF), the first step is to generate a random deviate from the Uniform distribution over the range $[0, 1]$ and then to use the inverse function to generate the random deviate.[7] This is the so-called inverse transform method.

We highlight the technique using the Logistic distribution, which has a readily invertible CDF. Its CDF is given by:

$$F(x) = \frac{1}{1 + e^{-(x-\mu)/s}}$$

where μ is the location parameter and s is the scale parameter. The inverse of the CDF, also known as the quantile function, is easily derived for any value of F, say p:

$$x = Q(p) = \mu + s \ln\left(\frac{p}{1-p}\right)$$

Figure 1 plots an example Logistic CDF with parameters $\mu = 9$ and $s = 3$. We randomly select 5 deviates from the Uniform distribution: $0.12, 0.36, 0.54, 0.79, 0.95$, visible along the y-axis. We then generate the random deviates for the Logistic distribution by locating the Uniform deviates on the y-axis of the CDF and evaluating the corresponding Logistic deviates, respectively 3.0, 7.3, 9.5, 13.0, and 17.8, easily derived from the Logistic quantile function.

[7] Not all CDF's have an easy expression for their corresponding quantile function, including the Normal distribution. In the case of the latter, the inverse error function is readily available in most software packages. The Beta distribution is an example where the inverse CDF is not readily available. In these cases, other numerical techniques are deployed to generate random deviates.

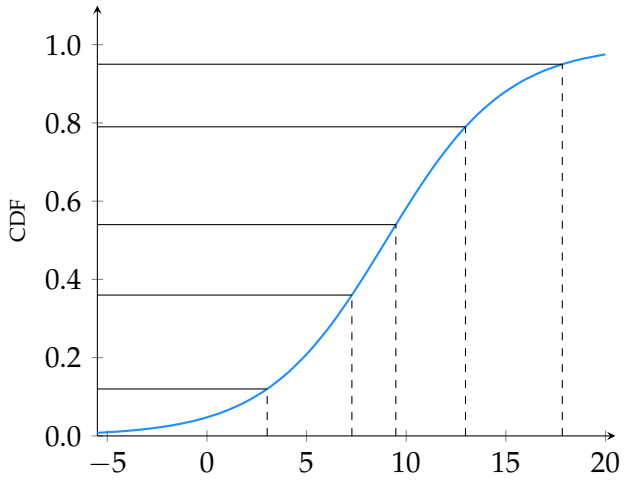

Figure 1. The Logistic distribution CDF and selecting random deviates

In the standard Monte Carlo method, a random deviate is sampled each time from the entire domain of the random variable, i.e., over $[0, 1]$. In the case of selecting a sample of 5, nothing guarantees that the sample will cover the full range. For example, 4 of the numbers could cluster around 0.65 with a fifth at 0.35. LHS sampling breaks the $[0, 1]$ range into 5 equal segments of width 0.2 (for a sample of 5). Sampling is done within each of the sub-ranges, guaranteeing that the sample will cover (almost) the entire range. In the more general case, with a sample size of n, LHS sampling divides the $[0, 1]$ range into equivalent sub-ranges with a width of $1/n$ and samples within the sub-ranges. The efficiency argument is that LHS allows to have a smaller sample size than standard Monte Carlo sampling, while ensuring that the full potential sample range is sampled. The technique is implemented for each random variable.

Figure 2 highlights a simple example of the potential benefits of LHS sampling.[8] The example uses the Logistic distribution with a location parameter of 0 and a scale parameter of 2. The mean of this distribution is 0 and the standard deviation is 3.628.[9] The x-axis of each graph, shows the number of draws for each sample, ranging from 50 to 5000 in steps of 50. The left-panel shows the deviation of the sample mean from the expected mean of 0 and the right-panel shows the percent deviation of the standard deviation from the expected standard deviation. Both figures clearly indicate that the LHS samples very quickly converge to the expected moments of the distribution. The Monte Carlo simulations show persistent deviations in the standard deviation, even with 5,000 draws.[10]

[8] The GAMS code that generates the data for the figure is available upon request.

[9] $\sigma = \sqrt{\frac{(\pi s)^2}{3}}$, where s is the scale parameter.

[10] The advantage of LHS sampling with many uncertain parameters is disputed, though part of the issue relates to memory and computer time, which is disappearing as an issue. A blog post

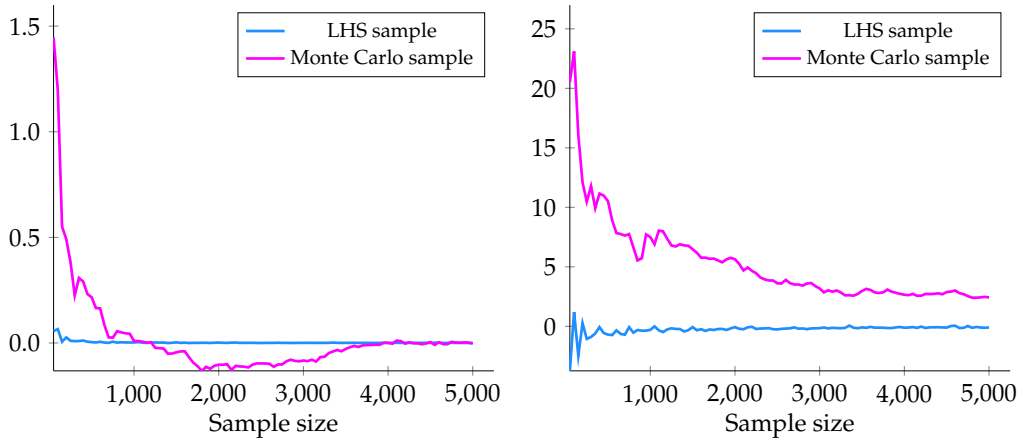

(a) Deviation from the expected mean (0)

(b) Deviation from expected standard deviation, %

Figure 2. Comparison of LHS versus Monte Carlo sampling for a Logistic(0,2) distribution

As coded in the LHS utility, the sample for each variable is in ascending order, as the samples are derived from each sub-range in ascending order. The deviates could be further randomized by sampling without replacement each of the deviates of each variable. The LHS utility does something a bit different. In the absence of user-specified correlations, it re-orders each column of deviates in such a way that the resulting correlation matrix across variables is (nearly) the identity matrix, while preserving the marginal distribution of each column. This is called the Iman-Conover method (Iman and Conover, 1982). The method is explained intuitively and with a numerical example in the Appendix. The same method is used if the user specifies a correlation matrix for all or some of the variables—a correlation of 0 is assumed for all pairs of variables for which a correlation is not user-provided.

In summary, the LHS method for Monte Carlo sampling, uses a method of stratified sampling, which is an efficient method to generate a sample that is nearly sure to cover the entire sample space. In addition, the deviates of each variable are ordered in such a way to (nearly) match a desired correlation scheme, which in the absence of any user-imposed correlations is the identity matrix.

2.2 An introduction to the LHS utility

The LHS utility is a program that generates a LHS sample based on a user-prepared input file describing the contours of the LHS cube: the list of random variables with their respective distributions and distribution parameters, and optionally correlations across pairs of the random variables. The input file is a simple text file and its contents is described in the Summary LHS User Guide (van der

by Lonnie Chrisman (https://lumina.com/latin-hypercube-vs-monte-carlo-sampling/) summarizes part of this discussion and provides additional references.

Mensbrugghe, 2023b). The output of the LHS utility is a data file containing the sample. The user has several output options including a CSV file, an XML file (readily loaded into Excel), a text-based GAMS data file and a GDX file.[11]

The LHS utility is a full recoding of the original utility, which has been developed in FORTRAN and can be downloaded from https://dakota.sandia.gov/downloads.[12] The re-coding has been done in C/C++ using mostly ANSI-C standards and thus should be readily compilable on other platforms, notably Linux and macOS.[13]

The two versions have been extensively tested and produce virtually the same sample.[14] The key advantage of the new version is the relative ease of coding in C/C++ compared with FORTRAN and the built-in memory management. While the FORTRAN code relies on a set of limits to the size of matrices, the C/C++ code uses dynamic memory management.[15]

The C/C++ version, in addition, has new features including additional distributions and new (and aforementioned) output options that facilitate embedding the utility in a workflow. The specific new features are:[16]

- Ten new distributions: Cauchy, Dagum, Fréchet, Gompertz, Gumbel, Laplace, Lévy, Logistic, Kumaraswamy and Rayleigh[17]
- Four additional output options: CSV, XML, GMS and GDX[18]
- A new optional random number generator based on the Mersenne Twister algorithm described in Matsumoto and Nishimura (1998) and Nishimura (2000)[19]

[11] The new software is fully backward compatible and the default output format is still supported.

[12] The download includes the full suite of software in Sandia National Lab's Dakota package. The LHS code is located in dakota-6.16.0-public-src-cli\packages\external\LHS. Interested users can contact the author for a copy of the FORTRAN code, which includes a few additional features and a *Makefile* to compile with GFortran.

[13] The new Mersenne Twister algorithm for generating random numbers requires a compiler that recognizes non-standard integer types, notably `unsigned long long`.

[14] The largest differences, and they are negligible, relate to deviates for the Beta distribution. The C/C++ code uses a different set of routines for the latter.

[15] The original FORTRAN code in fact crashed when attempting to generate the LHS sample for the IAM model. It had a relatively low limit on the number of potential user-based correlations.

[16] One feature that would be useful, but is not currently available, is an indexing feature—such as in modern packages, e.g., GEMPACK, GAMS, etc. In the case of the application described below, sampling is done for some 194 countries and each is output individually without the benefit of indexing. To alleviate some of the work in reading the sample, GAMS code is automatically generated in the workflow to facilitate the mapping of the variable definitions generated by the LHS code and indexed-based parameters in the GAMS code.

[17] The latest version of the FORTRAN code includes the Fréchet and Gumbel distributions.

[18] We also provide GEMPACK code that automates conversion of the CSV output into a GEMPACK HAR file.

[19] The version of this algorithm in the LHS code is explicitly based on a 64-bit architecture, which may limit its portability.

Table 1. Benchmarking of the LHS software

	Average seconds per sampling		Index relative to C/C++ with output	
	w/ output	w/o output	w/ output	w/o output
C/C++	8.4	6.0	1.0	0.7
FORTRAN	24.7	21.8	2.9	2.6

Most of the features of the LHS utility are described in the LHS User Guide (van der Mensbrugghe, 2023b). Users who are interested in the full features of the LHS utility (apart from the new ones) are referred to the original documentation in Swiler and Wyss (2004).

Benchmarking suggests that the C/C++ code is significantly faster than the FORTRAN code. Both are compiled with the Mingw compilers, so we would not expect to see such large differences. The benchmark involves sampling for the META 21 simulation described in the next section. The META 21 sample is large and with a significant number of correlated distributions.[20] The sampling is run 100 times for both the C/C++ and FORTRAN code. It is also run with and without saving the sample. The output file size is over 150MB, so it is possible that C/C++ is more efficient in writing than FORTRAN. The benchmarking results are summarized in Table 1. The FORTRAN version is around 2.9 times slower than the C/C++ code, and the speed difference is not linked to the writing of the output sample.

3. The Integrated Assessment Model

Integrated assessment models (IAMs) of climate change couple economic models that track GHG emissions with bio-physical models that at a minimum generate changes in the global mean temperature, which subsequently impact the economy via changes in economic potential such as crop yields, infrastructure, labor productivity, etc. Figure 3 provides a schema for the typical IAM model, which has four components: (1) the socio-economic module, which could be a CGE model, for example the GTAP model (Corong et al., 2017); or ENVISAGE (van der Mensbrugghe, 2019) (2) which generates emissions; (3) that impact atmospheric chemistry and the global energy balance, i.e., temperature; and (4) that impacts economic potential. In the context of ongoing research under the aegis of the Intergovernmental Panel on Climate Change (IPCC), most IAMs are using drivers and storylines called the shared socio-economic pathways (SSPs)—a set of five distinct storylines with variegated pathways for GDP and population growth.[21] The SSPs are coupled with the so-called Representative Concentration Pathways (RCPs)—that represent dif-

[20] The full sample is a matrix of dimension 10000×582 and a correlation matrix of dimension 582×582. The benchmark was done under Windows 10 under normal operations (on a non-synced drive) using an Intel i9 12th generation CPU and 64 GB of RAM.

[21] O'Neill et al. (2017) provides a description of the SSP narratives. The quantification in terms of population and GDP pathways for the 5 SSPs are described in KC and Lutz (2017) and Dellink et al. (2017), respectively.

ferent pathways for climate, with changes in the global mean temperature as one of the indicators.[22] The system will also be influenced by policies—mitigation polices that will change the emission pathways, and/or adaptation policies that will modify climate-induced impacts.

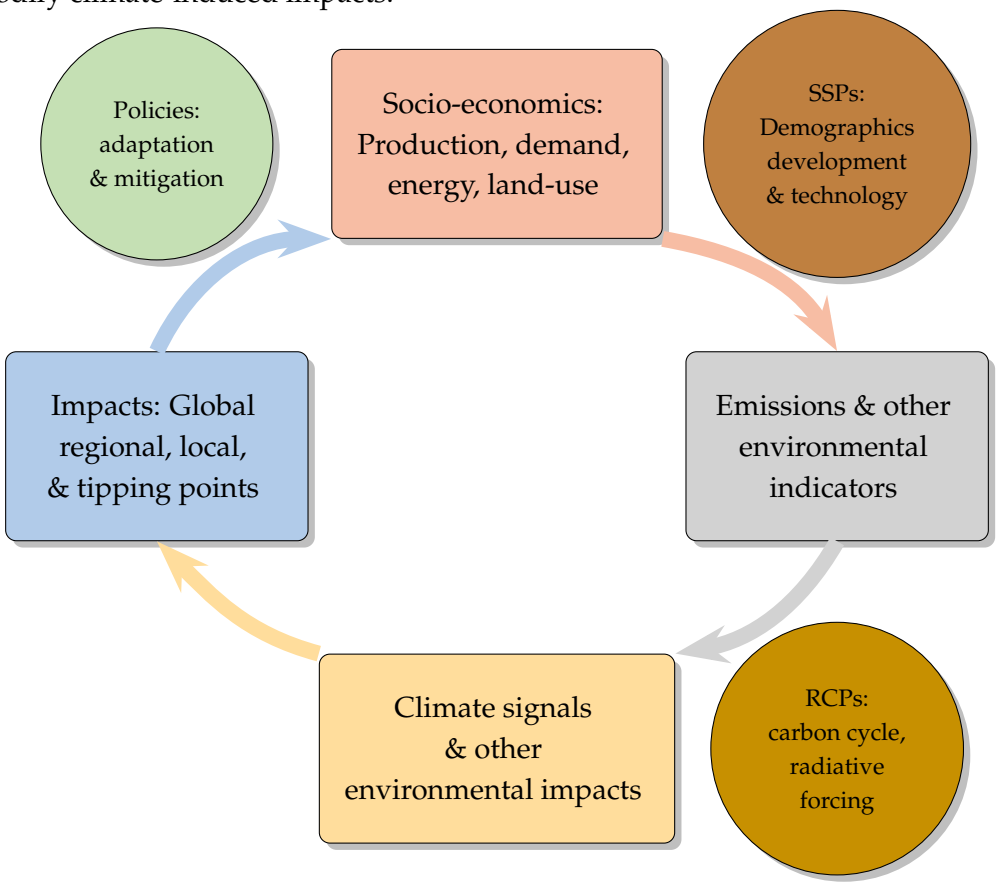

Figure 3. Integrated Assessment

This section is based one such IAM, the META 21 model (Dietz et al., 2021) and will be used to illustrate the coupling of the IAM with the LHS utility. The META 21 model is in the same spirit as Nordhaus' DICE/RICE suite of models (Nordhaus, 2017), Hope's PAGE model (Hope and Schaefer, 2016) and the FUND model (Anthoff and Tol, 2014).[23] Like these models, META 21 links emissions to the carbon cycle, to forcing and temperature change and then to economic damages. The economic and emissions module of the META 21 model are highly simplified and are largely exogenous in fact. GDP is driven by exogenous assumptions on total factor productivity (TFP) and savings and is only impacted by climate-induced

[22] See for example van Vuuren et al. (2011).

[23] Note that these three IAMs were the basis of the U.S. government's initial report on the so-called social cost of carbon (SCC), (Interagency Working Group on Social Cost of Carbon, 2016).

changes in TFP. Similarly, emissions are largely exogenous—not even responding to changes in GDP—though impacted by some of the modeled tipping points such as the release of methane from the oceans. Though small changes to GDP pathways will only have small impacts on emissions, a model such as META 21 is not able to assess mitigation pathways that require emissions to respond to economic incentives such as carbon pricing, subsidizing investment in carbon-free energy sources, etc.

This section will focus on only two parts of the META 21 model: (1) the energy balance model (EBM) that generates the change in global atmospheric temperature given the changes in emissions-induced radiative forcing; and (2) the ocean methane hydrate tipping point. The EBM section demonstrates the use of the LHS utility to provide correlated random deviates for the uncertain parameters of the EBM. The ocean methane hydrate tipping point section highlights how to generate random events in a simulation model.

A full description of META 21 and its parameterization is available in the supplementary materials of Dietz et al. (2021). A more cursory description of the full model and its implementation in GAMS and coupling with the LHS utility is provided in van der Mensbrugghe (2023a). While skipping a full description of META 21, the main features include:

1) The carbon cycle, radiative forcing and EBM are largely derived from the FaIR simple climate model.[24] One key innovation of the FaIR model, in terms of a simple representation of the carbon cycle was to introduce a time-varying parameter that enables capturing saturation effects, i.e., the ability to absorb carbon changes as concentrations of carbon evolve.
2) Changes in global mean surface temperature are down-scaled to country level.
3) META 21 incorporates a number of key bio-physical tipping points including:

    - The thawing of permafrost (PFC), which leads to additional carbon and methane emissions
    - The dissolution of methane hydrates (OMH) which leads to additional methane emissions
    - The Amazon dieback (AMAZ), which leads to a jump in carbon emissions
    - Ice sheet melting, which impacts sea-level rise. There are four sources of sea-level rise: thermal expansion, small ice-sheets and glaciers, the Greenland ice-sheet (GIS) and the West Antarctic ice-

[24]META 21 uses a relatively early version of FaIR (Millar et al., 2017). A newer, GAMS-based version, based on V2.0 (Leach et al., 2021) is available from the author. One of the innovations of V2.0 is the introduction of a 3-box version of the EBM, instead of a 2-box representation, to better capture transient temperature response.

sheet (WAIS)
- Modification of the Atlantic Meridional Overturning Circulation (AMOC), also called the thermohaline circulation. AMOC affects the change in country-level average temperatures
- The weakening of the Indian summer monsoon (ISM), which leads to an additional damage effect for India.

4) Captures changes in the planet's albedo from the change of ice cover—leading to adjustments in the change in the global mean surface temperature.
5) Interaction effects across the tipping points.
6) Damages that arise from rising temperatures and sea-level rise. Damages can impact GDP levels and/or GDP growth rates and the central estimates are based on recent research.
7) Calculates the social cost of carbon using a discounted utility indicator where the discount rate and pure rate of time preference are both subject to uncertainty.

The model captures two sources of uncertainty. The first source is the uncertainty in the model's parameters, for example the climate sensitivity parameter. META 21 captures this uncertainty with an explicit description of each parameter's probability distribution function (PDF), and in some cases also describes the correlation across parameter estimates, for example between equilibrium climate sensitivity and transitory climate sensitivity. This uncertainty is modeled using standard Monte Carlo techniques with random draws, albeit using the LHS methodology and targeting correlations across the uncertain parameters where identified. The second source of uncertainty deals with the start of the tipping points. In each future year, there is a non-zero probability that a tipping point starts. The probability itself increases with temperature. The event's start is sampled using the Binomial distribution with a single draw and the temperature-sensitive probability. Once an event starts, it is irreversible.

The original META 21 model is 'coded' in Excel and is linked to the Excel add-in @Risk software for the Monte Carlo draws. The Excel file contains the distribution information for the uncertain parameters, including their associated correlation assumptions. The draws for the start of events occur independently.[25]

The next section provides a deeper dive into two components of META 21—the EBM to demonstrate the use of LHS for the uncertain parameters and the ocean methane hydrates to demonstrate incorporation of modeling uncertain events.

[25] In principle, one could forego @Risk and use LHS to generate the sample of random deviates and link the relevant cells in the spreadsheet to the LHS-generated sample. The start of a random event can be generated with the Excel function `BINOM.INV(1, A2, RAND())`, where A2 represents the relevant probability. In essence this describes a Bernoulli trial with an outcome of 0 or 1. A macro would be needed to automate the running of the Monte Carlo simulations and save the desired results.

3.1 The Energy Balance Module

3.1.1 EBM specification

The energy balance model from DICE, FaIR and others can take the same matrix form:

$$T_t = [1 + A]\, T_{t-1} + M\, RF_t \tag{1}$$

where T represents the (change) in temperature in time t and is defined over two or more temperature boxes.[26] The only input to the EBM is the contemporaneous level of radiative forcing (and the lagged values of the change in temperature). In the case of DICE and FaIR 1.5 there are two boxes, essentially the atmosphere (and the surface and shallow ocean) and the (deep) ocean. In FaIR 2.0, the ocean box is split into shallow and deep. The matrix A represents the conveyance of energy across the boxes and the matrix M represents the impact of the contemporaneous radiative forcing on atmospheric temperature. In the FaIR 2.0 model, the matrix A takes the following form:

$$A = \begin{pmatrix} -(\lambda + \kappa_2)/C_1 & \kappa_2/C_1 & 0 \\ \kappa_2/C_2 & -(\kappa_2 + \varepsilon\kappa_3)/C_2 & \varepsilon\kappa_3/C_2 \\ 0 & \kappa_3/C_3 & -\kappa_3/C_3 \end{pmatrix}$$

where the parameter C is the heat capacity of each box, the κ parameters are the heat exchange coefficients, λ is a feedback parameter and ε allows to account for transient warming. M is a 3×1 vector with $1/C_1$ in the first cell.[27]

The META 21 model uses a two-box model, the parameterization of which will be described below. In the full model, the change in temperature derived from equation (1) is further adjusted by a factor influenced by the changing albedo.

3.1.2 EBM parameterization

The sampling strategy for the energy balance model parameters is provided in Table 2.[28] The sampled distribution modes line up well with the desired modes, with the largest deviation, around 1.1%, for the mean of the `C_0` parameter. Tables 3 and 4 provide, respectively, the targeted and sample correlations for the energy balance model parameters. The deviations between the two are not insignificant but are relatively good for the highly correlated parameters such as between

[26] It is a discrete approximation to the state-space form, which is $\dot{T} = A\, T + M\, RF$.

[27] The DICE parameterization can be converted to this matrix notation by setting κ_2 to `C3` (in the DICE code), λ is equal to `fco22x/t2xo2`, C_1 is equal to `1/C1`, C_2 is equal to `C3/C4` and κ_3 is 0.

[28] The parameter λ is equated to *f2xco2*/*ECS*, where *f2xco2* is known as the climate sensitivity parameter and is measured as the change in radiative forcing from a doubling of carbon concentration and *ECS* is the equilibrium climate sensitivity (also sometimes labeled as *t2xco2*).

`xi_3` and `f2xco2` and between `f2xco2` and `t2xco2`.

Table 2. Sampling assumptions for the forcing and EBM parameters

			Expected		Sample	
Parameter	LHS	Distribution	*mu*	σ	*mu*	σ
$1/C_1$	`xi_1`	`Pareto(5.9,0.116)`	0.14	0.029	0.14	0.029
C_2	`C_0`	`Pareto(1.7,53.0)`	128.0	∞	126.6	259.6
κ_2	`xi_3`	`Triangular(0.5,0.5,1.24)`	0.75	0.174	0.75	0.174
f2xco2	`f2xco2`	`Normal(3.46,0.437)`	3.46	0.437	3.46	0.437
ECS	`t2xco2`	`Normal(3.25,0.800)`	3.25	0.800	3.25	0.800

3.2 Ocean methane hydrates (OMH)

The ocean methane hydrates module is one of the bio-physical tipping points in META 21. Ocean methane hydrates are significant pockets of ice-like crystals of methane and water under the ocean surface that could be released with rising temperatures. The probability of the beginning of the release of methane from ocean methane hydrates is given in equation (2), where b_{OMH} is the so-called hazard rate. Given the probability, in each year t, a single random draw from the binomial distribution is taken with the given probability. The indicator function takes the value of 1 for every year subsequent to a positive draw, i.e., the release of the methane hydrate starts in the first year of the positive draw, and is assumed to be irreversible. This method for simulating random events could be applied to a number of other phenomena such as extreme weather events, recessions, etc.

Figure (4) depicts the probability density for a sample of 100,000 random draws for the range of temperature change from 0 to 3°C. The red line shows the level of the probability of the methane release starting for each change in temperature—it starts at 0 and rises to over 30% when the temperature change is 3°C. The mode of the PDF is at around 0.8-0.9°C. Given that the current estimated level of temperature change is already over 1°C, this parameterization implies a relatively early start to the release of the methane hydrates.

$$p_t^{OMH} = 1 - \exp\left(-b^{OMH} T_t^{atm}\right) \tag{2}$$

Table 3. Targeted correlations for the energy balance model parameters

	`xi_1`	`C_0`	`xi_3`	`f2xco2`	`t2xco2`
`xi_1`	1				
`C_0`	-0.0445	1			
`xi_3`	-0.4372	-0.1198	1		
`f2xco2`	0.0139	-0.0397	-0.4623	1	
`t2xco2`	-0.1934	-0.0802	0.0655	0.6512	1

Table 4. Sampled correlations for the energy balance model parameters

	xi_1	C_0	xi_3	f2xco2	t2xco2
xi_1	1				
C_0	-0.0184	1			
xi_3	-0.3383	-0.0528	1		
f2xco2	0.0095	-0.0064	-0.4505	1	
t2xco2	-0.1676	-0.0175	0.0623	0.6510	1

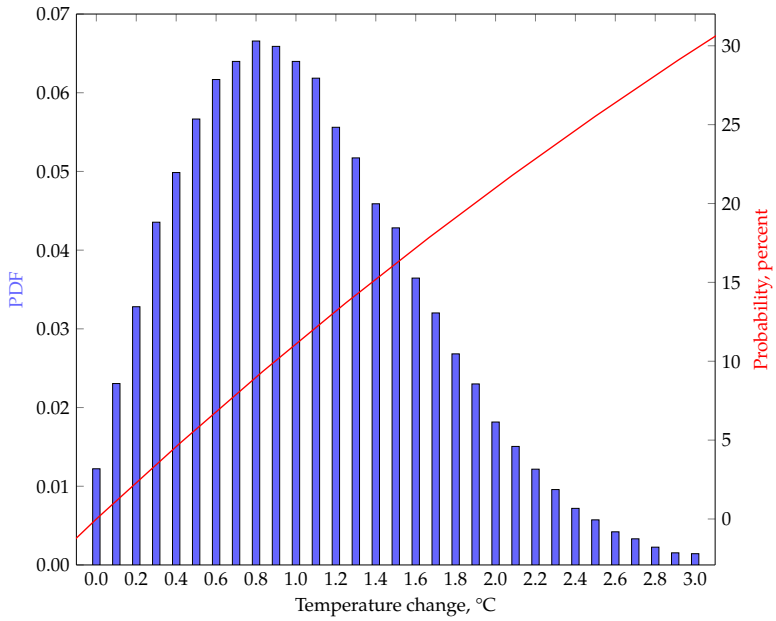

Figure 4. Sampling for OMH, where $b^{omh} = 0.118$

$$I_t^{OMH} = \begin{cases} 1 & \text{if } I_{t-1}^{OMH} = 1 \\ \texttt{randBinomial}(1, p_t^{OMH}) & \text{if } I_{t-1}^{OMH} = 0 \end{cases} \tag{3}$$

Once the emissions commence, a constant level of emissions is released each year until the given stock of sequestered methane runs out, equation (4), where $CH4_{Max}^{OMH}$ is the initial stock of sequestered methane and Δ^{OMH} is the annual release.

$$OMH_t = CH4_{Max}^{OMH} / \Delta^{OMH} \quad \text{if } I_t^{OMH} = 1 \text{ and } \sum_{t'=t_0}^{t-1} OMH_t < CH4_{Max}^{OMH} \tag{4}$$

4. An application

This section describes an application of the LHS tool coupled to the META 21 IAM model.

4.1 Sampling

The sampling is done with the LHS utility using the full distributional assumptions from the META 21 model. There are 9 uncertain parameters in the carbon cycle module—some of which have an identified correlation matrix; there are 6 uncertain parameters in the forcing and EBM module—again, some of which are assumed to be correlated; there are 8 independent uncertain tipping point parameters; and there are 3 uncertain parameters in the economic module. The damage module contains a very large number of uncertain parameters due to the fact that the damage parameters—of which there are three—are country specific. In addition the sampling takes into account the correlation matrix for the temperature-based damage coefficients. The input file for the LHS utility has over 75,000 lines in order to take into account the very large correlation matrix across the country-based temperature damage coefficients. Despite the size of the resulting LHS cube, the software operates in under 13 seconds. The resulting cube has 582 random variables sampled 10,000 times.

4.2 Results

This section describes some of the key results from the Monte Carlo simulations of the META 21 model—including assessing the relative role of including the tipping points in the analysis.

4.2.1 The social cost of carbon

With the current configuration for the simulations with tipping points, the simulation fails (for numerical) reasons for 183 observations, i.e., just under 2% of the sample size. Figure 5 presents the histogram for the remaining SCC values greater than 0 and less than $500. This removes some 17 negative values, of which 10 are less than $100 in absolute terms, and 51 values above $500, of which 6 are greater than $1000. There are also some unusual pairings and it might be useful to drill down to see if there are plausible explanations. For example, sample number 1885 has an SCC of $82 without the tipping points, but over $45,000 when the tipping points are included. Another extreme example is for sample number 8947. With tipping points, the SCC is -$89 and around -$6.5 million without the tipping points.

Figure 6 summarizes the SCC for the two configurations—with and without the tipping points. The median value of the SCC with tipping points is $60, and without tipping points is $48. The latter is somewhat lower than the value of $52 in Dietz et al. (2021), part of which could be attributed to differences in prices and exchange rates, we are using $2010 prices and purchasing power parity (PPP) ex-

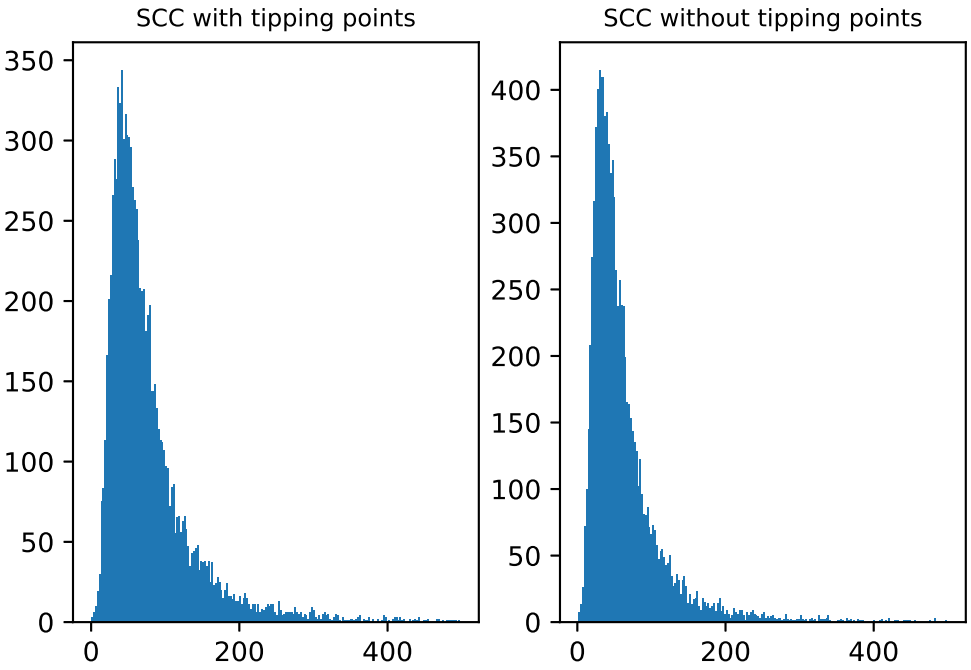

Figure 5. Histogram of SCC

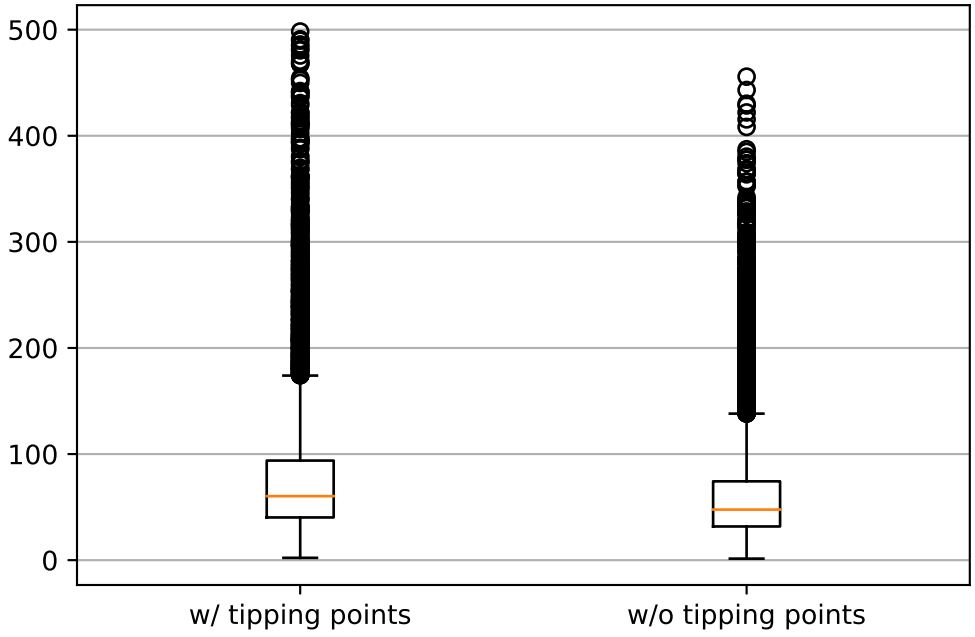

Figure 6. Box and whisker plot of SCC

change rates,[29] with the remainder attributable to changes in sampling strategy and removal of outliers. Thus, the inclusion of these tipping points raises the estimate of the SCC by around 26%, similar in magnitude to the increase in Dietz et al. (2021).

4.2.2 Tipping points start year

Table 5 describes the average start year for the uncertain tipping points. The parameterization assumes that the AMOC and OMH starting points are expected to start almost immediately, with the average start year for WAIS around 2058 and a much later start year for the Amazon dieback. The table also provides the frequency of the tipping point within the 2010/2200 time frame over the 10,000 samples. With the exception of the Amazon dieback, the tipping points are present in almost the entire sample, with the Amazon dieback occurring in roughly 50% of the samples. The distribution of the start years can be gleaned from Figure 7. The start years are heavily skewed towards the left, with the exception of the Amazon

[29] Dietz et al. (2021) inflate the SCC results by 20% to render the values in 2020 prices and exchange rates. Using the same factor would push our SCC value to $57.

Table 5. Tipping points start year

Tipping point	Average start year	Frequency
AMOC	2012	9749
OMH	2016	9743
WAIS	2058	9743
AMAZ	2110	4483

dieback, which has a relatively uniform distribution.[30]

4.2.3 Change in temperature

Figure 8 shows the change in temperature across the two configurations. The outer-most curves show the maximum and minimum temperature profiles across the 10,000 samples. The inner curves show the 95 percentile range. The middle curve shows the average. With the tipping points, the average temperature change could reach 4 °C by 2200, with a probability range between 2-6 °C, and a maximum of 10 °C. Without the tipping points, the ranges are more narrow—notably because 3 of the 5 tipping points have a direct impact on atmospheric concentrations of greenhouse gases.

4.2.4 Impacts on consumption

We conclude by assessing the impacts of damages and the tipping points on consumption. Figure 9 shows the average change in consumption in 2100 across countries relative to a no-damage baseline. There are a handful of countries that could benefit on average from rising temperatures—most visibly in the upper latitudes, e.g., Canada, Finland, Mongolia and Russia, but also China and the United States. The countries that would perceive the highest negative shocks are not visible as these are mostly small island nations. Other countries that would suffer damages in excess of 10% include Guyana and Suriname in South America, and Cameroon, Senegal, Sierra Leone, and Tunisia in Africa. The Netherlands, under these conditions, could see a fall of around 20%.

Figure 10 shows the impacts of excluding the tipping points in the assessment of the average damages. For the majority of countries, the impact of excluding the tipping points from the other damages would lead to a rise of per capita consumption in 2100 of between 0 and 2%. A few might actually benefit in relative terms from the tipping points, i.e., they are negatively impacted by excluding the tipping points—for example land-locked countries in Central Asia. The countries most impacted by the tipping points include the Netherlands, Jamaica, Bahrain, Sierra Leone, the Gambia, Guyana and Suriname. In the case of the Netherlands, exclusion of the tipping points raises per capita consumption by 8 percent relative to the full damage scenario (from a loss of 20% down to a loss of 12%). If these

[30] N.B. The x-axis differs across the tipping points.

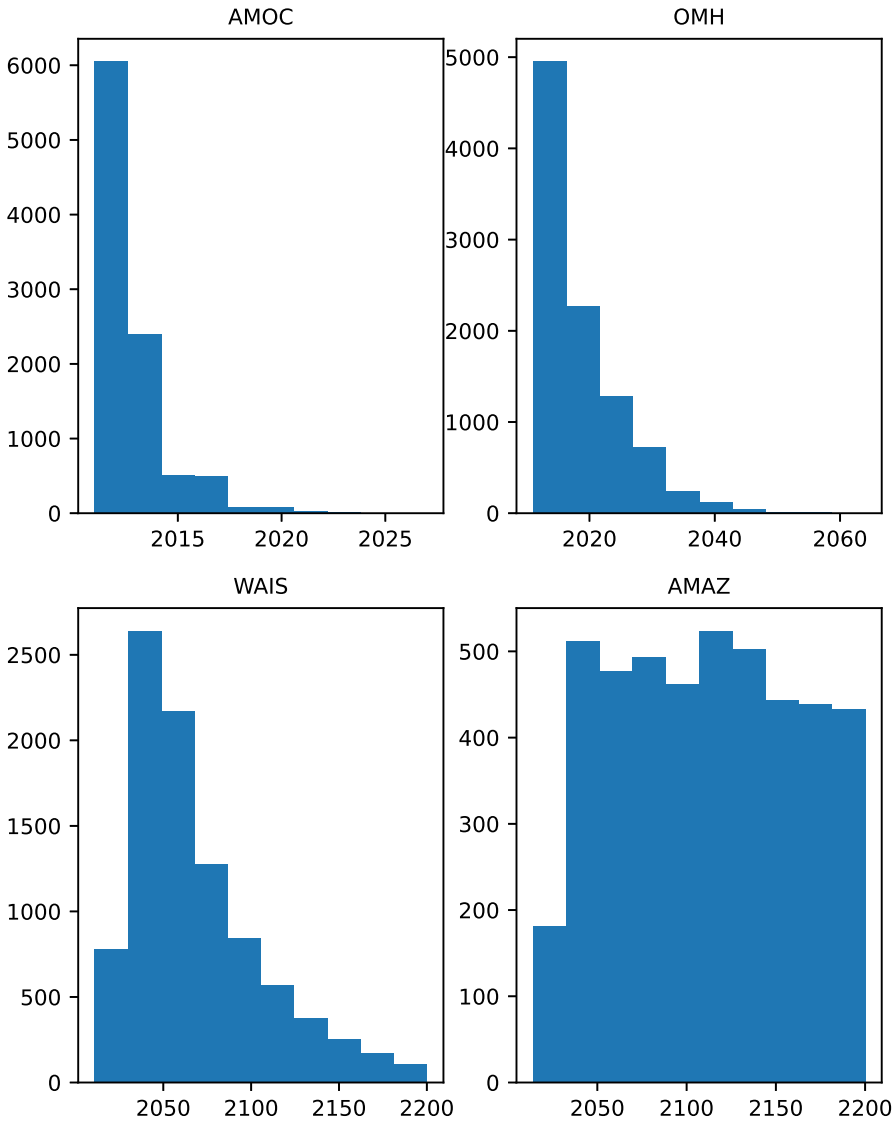

Figure 7. Tipping points start year

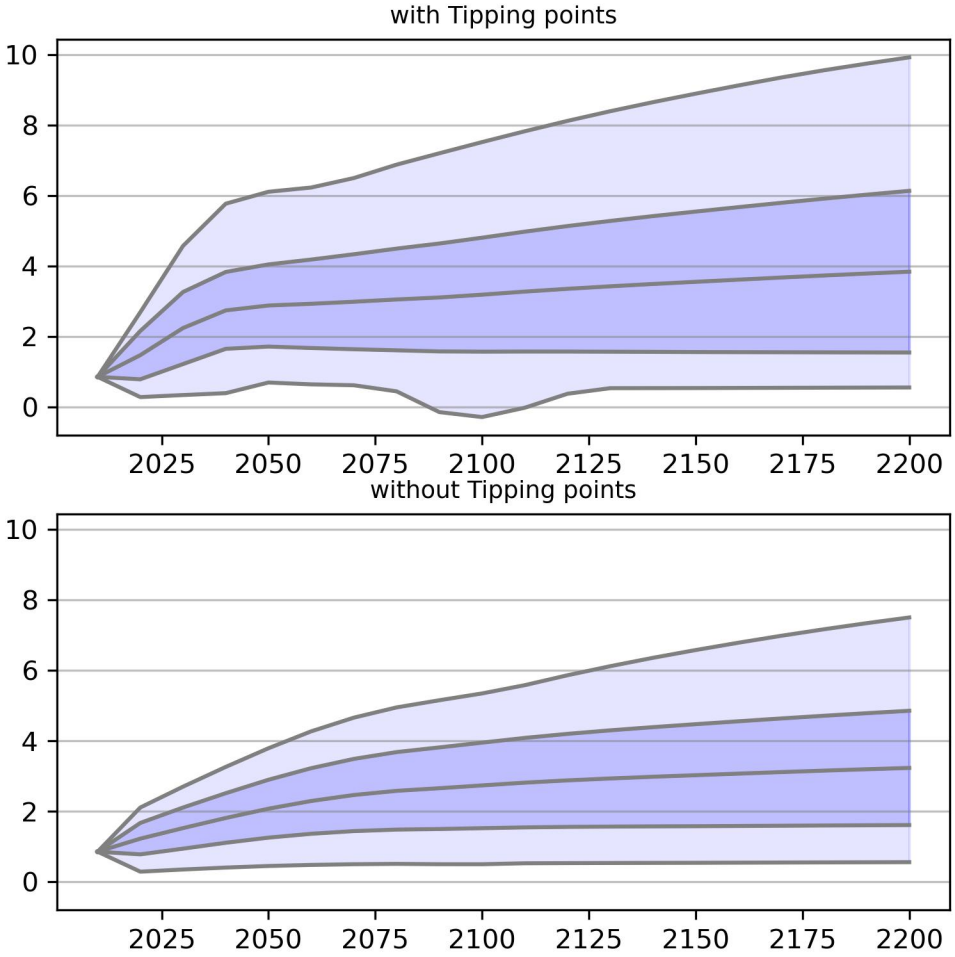

Figure 8. Change in temperature, °C

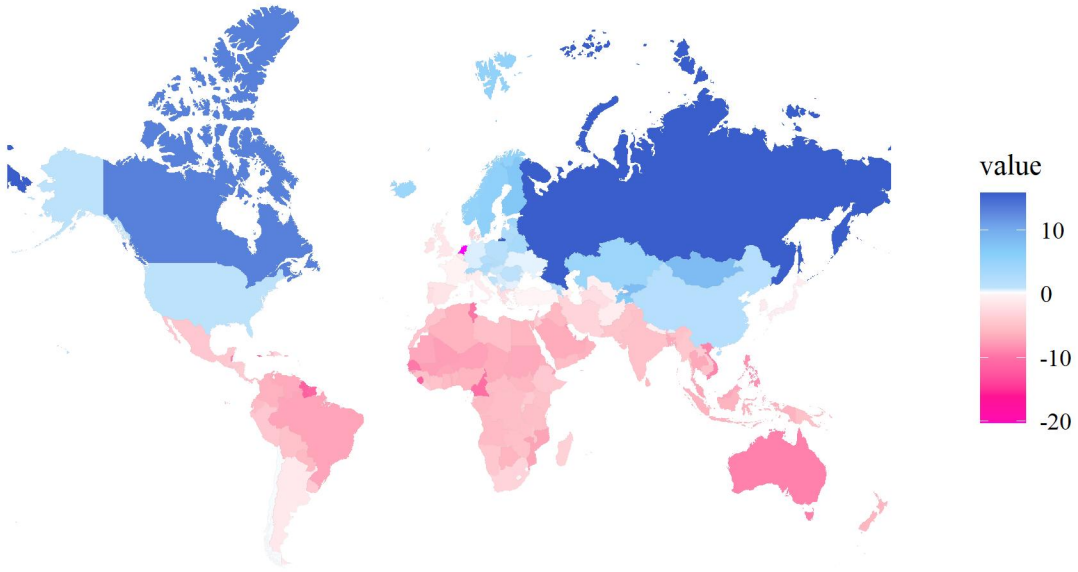

Figure 9. Average change in consumption in 2100 from climate change including tipping points, percent

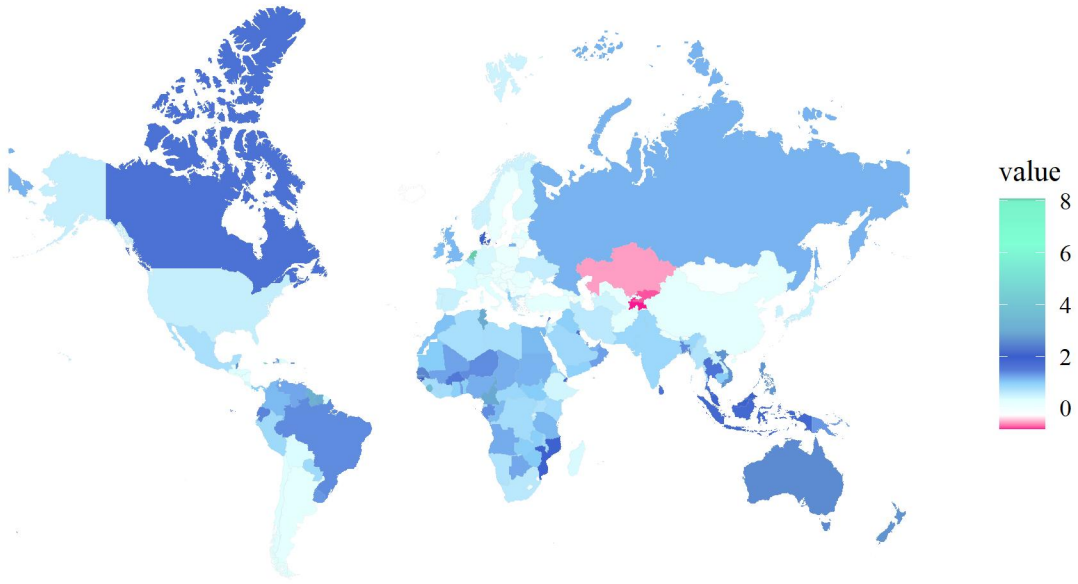

Figure 10. Average change in per capita consumption in 2100 when excluding tipping points, relative to the full damage scenario, percent

impacts are integrated in a more complex economic model, such as a CGE model, the impacts could be moderated by other *endogenous* mechanisms such as changing patterns of investment, production and trade.

5. Concluding remarks

This paper introduces a new version of a well-documented program, if perhaps little known among economists, to generate a Latin Hypercube Sample, including, if desired assumptions on the co-variability of the uncertain variables. The new program, coded in C/C++, has been tested exhaustively and also includes additional functionality compared with the original FORTRAN code, notably additional distributions and output options. The LHS utility can be readily embedded in a workflow, which links a simulation model with a Monte Carlo-style sample of random deviates with the desired distributional characteristics.

As an example, the LHS utility was coupled with the META 21 integrated assessment model (Dietz et al., 2021). The META 21 model has two distinct features related to Monte Carlo simulations. The first relates to a large number of uncertain parameters, for which the LHS utility was utilized to generate a random sample of 10,000 observations—including *a priori* assumptions for the correlations of a large

number of the uncertain parameters. The second relates to the uncertain timing of the onset of the specific tipping points, modeled using a hazard rate and a draw from a binomial distribution. Obviously, the LHS approach can be used in other contexts where uncertainty analysis can provide more robust conclusions than a single point estimate. Monte Carlo-type simulations have been used in the context of complex and large CGE models (Villoria (2017) and Villoria and Preckel (2017)) albeit with an analysis of only a small subset of the uncertainty of the parameter space or exogenous shocks. One advantage of the LHS approach over the GQ approach is that the sampling size is less sensitive to the number of uncertain parameters and the desired degree of capturing additional moments of the distribution.

There are many avenues for further exploration. Within the confines of the META 21 model, there are multiple configurations of the model, which could be used to unpack in greater depth the tipping points—alternative RCP/SSP combinations, the relative importance of specific tipping points, alternative specifications for any of the components of the model, etc. Beyond META 21, there are opportunities to port many of the components—notably the modeling of tipping points and the damage components, to other IAMs, including CGE models.[31] Finally, generation of random deviates that capture as broadly as possible the degree of uncertainty in the simulation framework is a necessary, but only first step in uncertainty analysis. Additional analysis is needed to determine the level of influence of uncertain parameters on key indicators—such as the social cost of carbon. This additional analysis could provide guidance on where to focus future research to reduce uncertainty. Examples of this type of analysis in the context of climate change include Lobell, Baldos, and Hertel (2013), Butler et al. (2014), Anderson et al. (2014) and Gillingham et al. (2018).

Acknowledgements

The initial development of this new version of the LHS utility was done a number of years ago while the author was working at the World Bank, so thanks to Hans Timmer who provided the space for its development. Needless to say, the delay in making the utility public is the author's alone. Let me also acknowledge help from Simon Dietz for elucidating some of the complexities of the META 21 model. A final thanks go to Steven Dirkse for helping with the parallelizing of the Monte Carlo simulations.

References

Anderson, B., E. Borgonovo, M. Galeotti, and R. Roson. 2014. "Uncertainty in Climate Change Modeling: Can Global Sensitivity Analysis Be of Help?" *Risk Anal-*

[31] The ENVISAGE Model (van der Mensbrugghe, 2019)—a GTAP-based recursive-dynamic IAM—has incorporated the FaIR 2.0 carbon cycles and EBM to endogenously determine temperature pathways. It would be fairly easy to include the META 21 tipping points.

ysis, 34(2): 271–293. doi:10.1111/risa.12117.

Anthoff, D., and R.S.J. Tol. 2014. "The Climate Framework for Uncertainty, Negotiation and Distribution (FUND), Technical Description, Version 3.9." Mimeo. http://www.fund-model.org/files/documentation/Fund-3-9-Scientific-Documentation.pdf.

Arndt, C. 1996. "An Introduction to Systematic Sensitivity Analysis via Gaussian Quadrature." Global Trade Analysis Project (GTAP), Department of Agricultural Economics, Purdue University, West Lafayette, IN, GTAP Technical Paper No. 2. https://www.gtap.agecon.purdue.edu/resources/res_display.asp?RecordID=305.

Butler, M.P., P.M. Reed, K. Fisher-Vanden, K. Keller, and T. Wagener. 2014. "Identifying parametric controls and dependencies in integrated assessment models using global sensitivity analysis." *Environmental Modelling & Software*, 59: 10–29. doi:10.1016/j.envsoft.2014.05.001.

Corong, E., T. Hertel, R. McDougall, M. Tsigas, and D. van der Mensbrugghe. 2017. "The Standard GTAP Model, Version 7." *Journal of Global Economic Analysis*, 2(1): 1–119. doi:10.21642/JGEA.020101AF.

Dellink, R., J. Chateau, E. Lanzi, and B. Magné. 2017. "Long-term economic growth projections in the Shared Socioeconomic Pathways." *Global Environmental Change*, 42: 200–214. doi:10.1016/j.gloenvcha.2015.06.004.

DeVuyst, E.A., and P.V. Preckel. 1997. "Sensitivity analysis revisited: A quadrature-based approach." *Journal of Policy Modeling*, 19(2): 175–185. doi:10.1016/0161-8938(95)00145-X.

Dietz, S., J. Rising, T. Stoerk, and G. Wagner. 2021. "Economic impacts of tipping points in the climate system." *Proceedings of the National Academy of Sciences*, 118(34). doi:10.1073/pnas.2103081118.

Fernando, R., W. Liu, and W.J. McKibbin. 2021. "Global economic impacts of climate shocks, climate policy, and changes in climate risk assessment." Brookings Institution, Washington, DC, Report. https://www.brookings.edu/wp-content/uploads/2021/03/20210331_CEEP_FernandoLiuMcKibbin_ClimateRisk_FINAL.pdf.

Gillingham, K., W. Nordhaus, D. Anthoff, G. Blanford, V. Bosetti, P. Christensen, H. McJeon, and J. Reilly. 2018. "Modeling Uncertainty in Integrated Assessment of Climate Change: A Multimodel Comparison." *Journal of the Association of Environmental and Resource Economists*, 5(4): 791–826. doi:10.1086/698910.

Helton, J.C., and F.J. Davis. 2002. "Latin Hypercube Sampling and the Propagation of Uncertainty in Analyses of Complex Systems." Sandia National Laboratories, Sandia Technical Report No. SAND2001-0417. doi:10.2172/806696.

Hope, C., and K. Schaefer. 2016. "Economic impacts of carbon dioxide and methane released from thawing permafrost." *Nature Climate Change*, 6: 56–59. doi:10.1038/nclimate2807.

Horridge, M., and K. Pearson. 2011. "Systematic Sensitivity Analysis with Re-

spect to Correlated Variations in Parameters and Shocks." Global Trade Analysis Project (GTAP), Department of Agricultural Economics, Purdue University, West Lafayette, IN, GTAP Technical Paper No. 30. https://www.gtap.agecon.purdue.edu/resources/res_display.asp?RecordID=3496.

Iman, R.L., and W.J. Conover. 1982. "A distribution-free approach to inducing rank correlation among input variables." *Communications in Statistics - Simulation and Computation*, 11(3): 311–334. doi:10.1080/03610918208812265.

Interagency Working Group on Social Cost of Carbon. 2016. "Technical Support Document: Technical Update of the Social Cost of Carbon for Regulatory Impact Analysis Under Executive Order 12866." United States Government, Report. https://www.epa.gov/sites/production/files/2016-12/documents/sc_co2_tsd_august_2016.pdf.

KC, S., and W. Lutz. 2017. "The human core of the shared socioeconomic pathways: Population scenarios by age, sex and level of education for all countries to 2100." *Global Environmental Change*, 42(42): 181–192. doi:10.1016/j.gloenvcha.2014.06.004.

Leach, N.J., S. Jenkins, Z. Nicholls, C.J. Smith, J. Lynch, M. Cain, T. Walsh, B. Wu, J. Tsutsui, and M.R. Allen. 2021. "FaIRv2.0.0: a generalised impulse response model for climate uncertainty and future scenario exploration." *Geoscientific Model Development*, 14(5): 3007–3036. doi:10.5194/gmd-14-3007-2021.

Lobell, D.B., U.L.C. Baldos, and T.W. Hertel. 2013. "Climate adaptation as mitigation: the case of agricultural investments." *Environmental Research Letters*, 8(1): 015012. doi:10.1088/1748-9326/8/1/015012.

Matsumoto, M., and T. Nishimura. 1998. "Mersenne Twister: A 623-Dimensionally Equidistributed Uniform Pseudo-Random Number Generator." *ACM Transactions on Modeling and Computer Simulation*, 8(1): 3–30. doi:10.1145/272991.272995.

McKay, M.D., R.J. Beckman, and W.J. Conover. 1979. "A Comparison of Three Methods for Selecting Values of Input Variables in the Analysis of Output from a Computer Code." *Technometrics*, 21: 239–245. doi:10.1080/00401706.1979.10489755.

Millar, R.J., Z.R. Nicholls, P. Friedlingstein, and M.R. Allen. 2017. "A modified impulse-response representation of the global near-surface air temperature and atmospheric concentration response to carbon dioxide emissions." *Atmospheric Chemistry and Physics*, 17(11): 7213–7228. doi:10.5194/acp-17-7213-2017.

Nishimura, T. 2000. "Tables of 64-Bit Mersenne Twisters." *ACM Transactions on Modeling and Computer Simulation*, 10(4): 348–357. doi:10.1145/369534.369540.

Nordhaus, W.D. 2017. "Revisiting the social cost of carbon." *Proceedings of the National Academy of Sciences*, 114(7). doi:10.1073/pnas.1609244114.

O'Neill, B.C., E. Kriegler, K.L. Ebi, E. Kemp-Benedict, K. Riahi, D.S. Rothman, B.J. van Ruijven, D.P. van Vuuren, J. Birkmann, K. Kok, M. Levy, and W. Solecki. 2017. "The roads ahead: Narratives for shared socioeconomic pathways describ-

ing world futures in the 21st century." *Global Environmental Change*, 42: 169–180. doi:10.1016/j.gloenvcha.2015.01.004.

Pauw, K., J. Thurlow, M. Bachu, and D.E. van Seventer. 2011. "The economic costs of extreme weather events: a hydrometeorological CGE analysis for Malawi." *Environment and Development Economics*, 16(2): 177–198. doi:10.1017/S1355770X10000471.

Pearson, K., and C. Arndt. 2000. "Implementing Systematic Sensitivity Analysis Using GEMPACK." Global Trade Analysis Project (GTAP), Department of Agricultural Economics, Purdue University, West Lafayette, IN, GTAP Technical Paper No. 3. https://www.gtap.agecon.purdue.edu/resources/res_display.asp?RecordID=474.

Swiler, L.P., and G.D. Wyss. 2004. "A User's Guide to Sandia's Latin Hypercube Sampling Software: LHS UNIX Library Standalone Version." Sandia National Laboratories, Sandia Technical Report No. SAND2004-2439. doi:10.2172/919175.

van der Mensbrugghe, D. 2019. "The Environmental Impact and Sustainability Applied General Equilibrium (ENVISAGE) Model. Version 10.01." Center for Global Trade Analysis (GTAP), Department of Agricultural Economics, Purdue University, West Lafayette, IN, Unpublished manuscript. https://mygeohub.org/groups/gtap/envisage-docs.

van der Mensbrugghe, D. 2023a. "The META 21 Integrated Assessment Model in GAMS and LHS Sampling." Global Trade Analysis Project (GTAP), Department of Agricultural Economics, Purdue University, West Lafayette, IN, GTAP Working Paper No. 95. https://www.gtap.agecon.purdue.edu/resources/res_display.asp?RecordID=7036.

van der Mensbrugghe, D. 2023b. "A Summary Guide to the Latin Hypercube Sampling (LHS) Utility." Global Trade Analysis Project (GTAP), Department of Agricultural Economics, Purdue University, West Lafayette, IN, GTAP Working Paper No. 94. https://www.gtap.agecon.purdue.edu/resources/res_display.asp?RecordID=7035.

van der Mensbrugghe, D. 2023c. "Using Python for Parallelization." Global Trade Analysis Project (GTAP), Department of Agricultural Economics, Purdue University, West Lafayette, IN, GTAP Working Paper No. 93. https://www.gtap.agecon.purdue.edu/resources/res_display.asp?RecordID=6826.

van Vuuren, D.P., J. Edmonds, M. Kainuma, K. Riahi, A. Thomson, K. Hibbard, G.C. Hurtt, T. Kram, V. Krey, J.F. Lamarque, T. Masui, M. Meinshausen, N. Nakicenovic, S.J. Smith, and S.K. Rose. 2011. "The representative concentration pathways: an overview." *Climatic Change*, 109: 5–31. doi:10.1007/s10584-011-0148-z.

Villoria, N.B. 2017. "R Meets GEMPACK for a Monte Carlo Walk." *Journal of Global Economic Analysis*, 2(2): 128–154. doi:10.21642/JGEA.020204AF.

Villoria, N.B., and P.V. Preckel. 2017. "Gaussian Quadratures vs. Monte Carlo Experiments for Systematic Sensitivity Analysis of Computable General Equilib-

rium Model Results." *Economics Bulletin*, 37(1): 480–487.

Appendix A. The LHS algorithm

The origin of LHS is attributed to the work of McKay (McKay, Beckman, and Conover, 1979) and Iman and Conover (Iman and Conover, 1982), which is very nicely described by Helton and Davis (Helton and Davis, 2002). LHS has two components. The first is intended to cover as much of the sampling space as possible by using a simplified version of stratified sampling. The key idea behind this is to reduce the number of samples—particularly for complex models. In random sampling, each random deviate is selected over the entire range of possible outcomes, i.e., over the probability range of $[0, 1]$. The LHS technique divides the $[0, 1]$ range into n sub-intervals of equal length set to $1/n$, where n is the number of deviates being requested in the sample. In this sense, LHS covers the entire probability range. For example, for a sample size of 10, the procedure is certain to select a deviate from the $[0, 0.1]$, whereas their is no guarantee of this outcome from pure random sampling. This simplified stratified sampling is used for each random variable, and hence LHS is sure to cover the entire range of the multi-variate sample.

The second component is the pairing of the deviates so as to match a targeted correlation matrix for the random variables. In the absence of a user-specified correlation matrix, the algorithm pairs the deviates to target a zero-correlation matrix, or as close as possible. The pairing part of the algorithm has several components, which are described below. Let X be a matrix of the initial random deviates. It is of dimension $n \times k$, where n is the sample size and k is the number of random variables. Given the sampling strategy, each column of X is sorted in ascending order. Let C be the targeted correlation matrix, in the absence of a user-specified list of correlations, it is the identity matrix. It has the dimensions of $k \times k$, is symmetric and semi-positive definite. Therefore, it can be split using the Cholesky factorization, which is a lower triangular matrix, say H, with the property $C = HH'$.[32]

The second step involves developing an auxiliary matrix of random deviates, based on the so-called van der Waerden scores. This matrix will be transformed such that it has the same correlation as the target correlation, and once this is accomplished, its rank scores will be used to derive the same rank for the original sample.

The van der Waerden scores represent the inverse of the normal standard deviation and each column will have the same initial distribution, until fully randomized. For example, in the case of $n = 10$, each column has the following values until randomized:

[32] Horridge and Pearson (2011) use a similar technique for their method of systematic sensitivity analysis using Gaussian quadrature and allowing for imposing a covariance matrix on the uncertain parameters.

$$\begin{bmatrix} -1.335178 \\ -0.908458 \\ -0.604585 \\ -0.348756 \\ -0.114185 \\ 0.114185 \\ 0.348756 \\ 0.604585 \\ 0.908458 \\ 1.335178 \end{bmatrix}$$

which is the inverse of the cumulative distribution function of the standard normal distribution at each cumulative interval defined by $1/11$. After randomization, column by column, the matrix S, may look something like the following:

$$S = \begin{bmatrix} -0.11419 & -1.33518 & -0.34876 & -0.34876 & 0.90846 \\ 0.11419 & 0.34876 & 0.11419 & 0.34876 & -0.90846 \\ -0.90846 & 0.60459 & -0.90846 & -0.60459 & 0.60459 \\ -1.33518 & 0.11419 & 0.60459 & -0.90846 & -0.34876 \\ 0.90846 & -0.60459 & -1.33518 & -0.11419 & -0.11419 \\ 0.60459 & -0.34876 & 0.34876 & 0.90846 & 1.33518 \\ -0.34876 & 1.33518 & -0.60459 & 1.33518 & -1.33518 \\ 1.33518 & -0.11419 & 0.90846 & -1.33518 & -0.60459 \\ 0.34876 & 0.90846 & 1.33518 & 0.11419 & 0.11419 \\ -0.60459 & -0.90846 & -0.11419 & 0.60459 & 0.34876 \end{bmatrix}$$

for a sample of 5 random variables. From the matrix S, which to emphasize, has nothing to do with the sample itself, we can derive its correlation matrix $C^s = Corr(S)$, and the subsequent Cholesky decomposition ($C^s = H^s \left(H^s\right)'$) and the inverse of the Cholesky decomposition, call the latter $M = \left(H^s\right)^{-1}$. The following step transforms S to S^1:

$$S^1 = S \left(HM\right)'$$

where $\left(HM\right)'$ is a projection matrix, based on the targeted Cholesky matrix and the inverse of the Cholesky matrix derived from the van der Waerden scores. S^1 it turns out will have the desired correlation matrix, i.e., its correlation matrix will be C, the targeted correlation matrix. The final step is to assume that the matrix S^1, of transformed van der Waerden scores, has the same rank correlation as the sample of random deviates. So the algorithm proceeds to calculate the rank order of each

Table A.1. Example of a sample definition for an EBM model

Name	Distribution	Parm 1	Parm 2	Parm 3
xi_1	Pareto	5.907	0.11628	
C_0	ParetoAlt	1.7062	53.0	
xi_3	Triangular	0.5	0.5	1.23723
f2xco2	Normal	3.45938	0.43674	
t2xco2	Normal	3.25312	0.80031	

column of S^1 and uses that rank order to re-order the cells in each column of X.

The following numerical example will show how the algorithm works in practice. The example is for a set of five random variables with the attributes in Table A.1. This is an example for the energy balance model (EBM) of the META 21 model, which drives the change in temperature component. In addition, the components are assumed to be linked to a correlation matrix as below.

$$C = \begin{bmatrix} & xi\_1 & C\_0 & xi\_3 & f2xco2 & t2xco2 \\ xi\_1 & 1.00000 & & & & \\ C\_0 & -0.04451 & 1.00000 & & & \\ xi\_3 & -0.43716 & -0.11978 & 1.00000 & & \\ f2xco2 & 0.01392 & -0.03966 & -0.46228 & 1.00000 & \\ t2xco2 & -0.19343 & -0.08016 & 0.06549 & 0.65122 & 1.00000 \end{bmatrix}$$

The targeted Cholesky matrix is given by:

$$H = \begin{bmatrix} & xi\_1 & C\_0 & xi\_3 & f2xco2 & t2xco2 \\ xi\_1 & 1.00000 & & & & \\ C\_0 & -0.04451 & 0.99901 & & & \\ xi\_3 & -0.43716 & -0.13937 & 0.88852 & & \\ f2xco2 & 0.01392 & -0.03907 & -0.51956 & 0.85343 & \\ t2xco2 & -0.19343 & -0.08886 & -0.03540 & 0.74060 & 0.63635 \end{bmatrix}$$

The initial sample of random deviates is given below.[33] The rank correlation is exactly 1 for all pairs of columns as all of the deviates are in ascending order in each column, and the Spearman correlation matrix is also nearly the identity matrix.

[33] This will depend on the random sample function and the initial seed.

$$X = \begin{bmatrix} xi\_1 & C\_0 & xi\_3 & f2xco2 & t2xco2 \\ 0.11646 & 56.14932 & 0.51226 & 2.63749 & 2.11869 \\ 0.11920 & 59.22047 & 0.55074 & 3.05827 & 2.28394 \\ 0.12332 & 65.15213 & 0.58688 & 3.13678 & 2.81773 \\ 0.12652 & 65.61294 & 0.62132 & 3.32291 & 2.85096 \\ 0.12781 & 77.97449 & 0.67191 & 3.45491 & 3.10905 \\ 0.13417 & 82.40018 & 0.76344 & 3.52562 & 3.39424 \\ 0.14078 & 95.69734 & 0.79359 & 3.60265 & 3.55156 \\ 0.14771 & 108.00303 & 0.87995 & 3.78290 & 3.91509 \\ 0.15354 & 153.88674 & 0.94936 & 3.89073 & 3.92973 \\ 0.17777 & 272.65331 & 1.07535 & 4.59178 & 4.34054 \end{bmatrix}$$

The correlation matrix for S is given by:

$$C^s = \begin{bmatrix} & xi\_1 & C\_0 & xi\_3 & f2xco2 & t2xco2 \\ xi\_1 & 1.00000 & & & & \\ C\_0 & -0.16433 & 1.00000 & & & \\ xi\_3 & 0.16526 & 0.17962 & 1.00000 & & \\ f2xco2 & -0.04612 & 0.21876 & -0.21009 & 1.00000 & \\ t2xco2 & -0.01611 & -0.56745 & -0.03087 & -0.03345 & 1.00000 \end{bmatrix}$$

and the corresponding Cholesky matrix is:

$$H^s = \begin{bmatrix} & xi\_1 & C\_0 & xi\_3 & f2xco2 & t2xco2 \\ xi\_1 & 1.00000 & & & & \\ C\_0 & -0.16433 & 0.98641 & & & \\ xi\_3 & 0.16526 & 0.20963 & 0.96371 & & \\ f2xco2 & -0.04612 & 0.21409 & -0.25666 & 0.94136 & \\ t2xco2 & -0.01611 & -0.57795 & 0.09644 & 0.12141 & 0.80104 \end{bmatrix}$$

from which we derive the inverse matrix:

$$M = \begin{bmatrix} & xi\_1 & C\_0 & xi\_3 & f2xco2 & t2xco2 \\ xi\_1 & 1.00000 & & & & \\ C\_0 & 0.16660 & 1.01378 & & & \\ xi\_3 & -0.20772 & -0.22052 & 1.03765 & & \\ f2xco2 & -0.04553 & -0.29068 & 0.28292 & 1.06229 & \\ t2xco2 & 0.17222 & 0.80205 & -0.16781 & -0.16101 & 1.24837 \end{bmatrix}$$

We now have all the elements to transform the S matrix:

$$S^1 = S\,(HM)' = \begin{bmatrix} xi\_1 & C\_0 & xi\_3 & f2xco2 & t2xco2 \\ -0.11419 & -1.36616 & 0.20236 & 0.01005 & 0.19013 \\ 0.11419 & 0.36713 & -0.08598 & 0.23054 & -0.41555 \\ -0.90846 & 0.50155 & -0.45556 & -0.45183 & 0.24884 \\ -1.33518 & -0.04715 & 1.38002 & -1.12544 & -0.66758 \\ 0.90846 & -0.50155 & -1.61302 & 0.46806 & -0.49921 \\ 0.60459 & -0.27950 & 0.04923 & 0.82639 & 1.55553 \\ -0.34876 & 1.30972 & -0.78274 & 1.13261 & 0.14081 \\ 1.33518 & 0.04715 & 0.01497 & -1.35900 & -1.52515 \\ 0.34876 & 0.96259 & 0.69972 & -0.42452 & 0.40673 \\ -0.60459 & -0.99378 & 0.59100 & 0.69313 & 0.56545 \end{bmatrix}$$

The correlation matrix of S^1 matches the targeted correlation matrix for the sample. The rank ordering of each of the columns of S^1 is given by:

$$R^1 = \begin{bmatrix} xi\_1 & C\_0 & xi\_3 & f2xco2 & t2xco2 \\ 5 & 1 & 7 & 5 & 6 \\ 6 & 7 & 4 & 6 & 4 \\ 2 & 8 & 3 & 3 & 7 \\ 1 & 5 & 10 & 2 & 2 \\ 9 & 3 & 1 & 7 & 3 \\ 8 & 4 & 6 & 9 & 10 \\ 4 & 10 & 2 & 10 & 5 \\ 10 & 6 & 5 & 1 & 1 \\ 7 & 9 & 9 & 4 & 8 \\ 3 & 2 & 8 & 8 & 9 \end{bmatrix}$$

Based on R^1, we re-arrange the rows of X to yield:

$$X^1 = \begin{bmatrix} xi\_1 & C\_0 & xi\_3 & f2xco2 & t2xco2 \\ 0.12781 & 56.14932 & 0.79359 & 3.45491 & 3.39424 \\ 0.13417 & 95.69734 & 0.62132 & 3.52562 & 2.85096 \\ 0.11920 & 108.00303 & 0.58688 & 3.13678 & 3.55156 \\ 0.11646 & 77.97449 & 1.07535 & 3.05827 & 2.28394 \\ 0.15354 & 65.15213 & 0.51226 & 3.60265 & 2.81773 \\ 0.14771 & 65.61294 & 0.76344 & 3.89073 & 4.34054 \\ 0.12652 & 272.65331 & 0.55074 & 4.59178 & 3.10905 \\ 0.17777 & 82.40018 & 0.67191 & 2.63749 & 2.11869 \\ 0.14078 & 153.88674 & 0.94936 & 3.32291 & 3.91509 \\ 0.12332 & 59.22047 & 0.87995 & 3.78290 & 3.92973 \end{bmatrix}$$

which is the final sample. Each column has the same sample distribution as the corresponding column in X, but the deviates have been arranged so that the correlation matrix is 'near' the targeted correlation matrix. In this case, the correlation matrix is:

$$C^1 = \begin{bmatrix} & xi\_1 & C\_0 & xi\_3 & f2xco2 & t2xco2 \\ xi\_1 & 1.00000 & & & & \\ C\_0 & -0.17602 & 1.00000 & & & \\ xi\_3 & -0.31037 & -0.26483 & 1.00000 & & \\ f2xco2 & -0.32630 & 0.55056 & -0.29066 & 1.00000 & \\ t2xco2 & -0.26453 & 0.00238 & 0.12102 & 0.45300 & 1.00000 \end{bmatrix}$$

The 'fit' is not so good in this example, in part because the sample size is very small. Using the LHS tool with a sample size of 20,000, we get the following correlation matrix. Though not exactly the target, it is much closer than that with the sample size of 10. As explained in Swiler and Wyss (2004), there are limitations on the targeted correlations.

$$C^2 = \begin{bmatrix} & xi\_1 & C\_0 & xi\_3 & f2xco2 & t2xco2 \\ xi\_1 & 1.00000 & & & & \\ C\_0 & -0.04270 & 1.00000 & & & \\ xi\_3 & -0.42080 & -0.11510 & 1.00000 & & \\ f2xco2 & 0.01130 & -0.04040 & -0.44650 & 1.00000 & \\ t2xco2 & -0.18610 & -0.07590 & 0.05960 & 0.63470 & 1.00000 \end{bmatrix}$$